ELSEVIER

Carbohydrate Research 268 (1995) 159–175

CARBOHYDRATE RESEARCH

Dynamics in aqueous solutions of the pentasaccharide corresponding to the binding site of heparin for antithrombin III studied by NMR relaxation measurements [1,2]

Miloš Hricovíni *, Giangiacomo Torri

Istituto di Chimica e Biochimica G. Ronzoni, via G. Colombo 81, I-20133 Milano, Italy

Received 28 June 1994; accepted 13 October 1994

Abstract

^{1}H NMR and ^{13}C NMR relaxation measurements at different magnetic field strengths were used to study the nature of overall and internal motions, in aqueous solution, of the synthetic pentasaccharide (A-G-A*-I-A_M) corresponding to the binding site of heparin for antithrombin III. Two-dimensional double INEPT spectra were recorded at 11.7 T with and without suppression of cross-correlation effects between dipolar and chemical shift anisotropy relaxation mechanisms in measurements of spin-lattice and spin-spin relaxation times. Moreover, longitudinal relaxation times were collected at 7 T with the inversion recovery method. One dimensional NOESY spectra were recorded at 11.7 T and 9.4 T with various mixing times when spins of the A1* and A4* protons were inverted in the central residue of the pentasaccharide. Differences in the T_1 relaxation times, as well as in the cross-relaxation rates between protons relaxing through fixed distances in the A* residue, indicated that the molecule tumbles anisotropically in solution. However, in order to achieve agreement between the spectral and the model data, the presence of internal motions had to be also considered, in addition to the assumption of a symmetric top model for the description of overall tumbling. The changes in the longitudinal and transversal relaxation times, collected with and without suppression of interference effects, supported the assumption that the cross-correlation between dipolar and chemical shift anisotropy relaxation mechanisms cannot be neglected in this medium-sized molecule. In fact, the influence of these effects was

* Corresponding author. Institute of Chemistry, Slovak Academy of Sciences, SK-84238 Bratislava, Slovakia

[1] This paper is dedicated to the memory of Professor Jean Choay.

[2] Presented at the 3rd International Satellite Meeting on the Conformational Analysis of Carbohydrates and Protein/Carbohydrate Interactions, July 24–28, 1994, Val Morin, Canada,

SSDI 0008-6215(94)00334-3

10–15% in T_1 and 20–25% in T_2 relaxation times. The experimental data were analyzed using model free formalism and the computed order parameters indicate a decrease in spatial restriction from the central residue ($S^2 \sim 0.9$) towards both ends of the pentasaccharide ($S^2 \sim 0.7$). The anisotropy ratio found was ~ 3.3 with correlation times $\tau_{\parallel} = 450$ ps and $\tau_{\perp} = 1480$ ps. The values of effective correlation time were within the range of tens of picoseconds. Thus, for a more precise interpretation of the experimental data for the pentasaccharide, in addition to internal motions and anisotropic tumbling, the effect of cross-correlation must be taken into account as well.

Keywords: Pentasaccharide; NMR relaxation; Internal motions; Anisotropic tumbling; Cross-correlation effect

1. Introduction

Nuclear magnetic resonance relaxation measurements provide valuable information about the dynamics of biologically active substances in solution [1]. One can obtain, at least in principle, a comprehensive picture of the overall tumbling and internal motions in molecules. Both homo- and hetero-nuclear relaxation measurements have been used, and the heteronuclear two-dimensional [2] proton-detected spectroscopy [3] has been shown to be useful owing to its increased sensitivity and resolution, especially for studies of nuclei with low gyromagnetic ratio at natural abundance. Internal motions in picosecond and nanosecond time scales are present in various proteins [4] with amplitudes significantly larger than originally assumed. Though most studies have so far focussed on protein structure and dynamics, there is increasing evidence of important biological functions of various oligo- and poly-saccharides, and this has stimulated interest in this field. Experimental NMR studies on carbohydrate conformation have also utilized relaxation measurements [5]. According to several studies [6] blood group oligosaccharides and some other biologically important carbohydrates adopt a single conformation. However, significant internal motions in oligosaccharides have also been described [7]. For some disaccharides, the rate of internal motions about the glycosidic linkage was found to be comparable with overall tumbling [8].

Glycosaminoglycans are co-polymers of uronic acid and a hexosamine. They are widely distributed in animal tissues and have important biological functions – they control cell growth and differentiation of cellular metabolism, play an important role in defence mechanisms against infections, and they showed antiangiogenic and antitumor activities [9]. More specifically, the sulfated, L-iduronic acid containing polysaccharide heparin is of great therapeutic interest. It has been shown [10] that it specifically binds to the plasma protein antithrombin III, leading to anticoagulant and antithrombotic activity. Even a short and very specific part of heparin – pentasaccharide **I** (Scheme 1) has comparable affinity to antithrombin III, like that of the polysaccharide itself. Early NMR studies on heparin and pentasaccharide structures showed considerable discrepancies among the experimental three-bond proton–proton coupling constants in the L-iduronic unit and those expected on the basis of $^1C_4$ or $^4C_1$ chair forms of this residue [11]. This disagreement has been explained by the existence of three conformers in equilibrium in heparin, $^1C_4$, $^4C_1$, and $^2S_0$ [12] and confirmed experimentally by strong NOE interaction between H-2 and H-5 protons in the L-iduronic unit [13] as well as by molecular

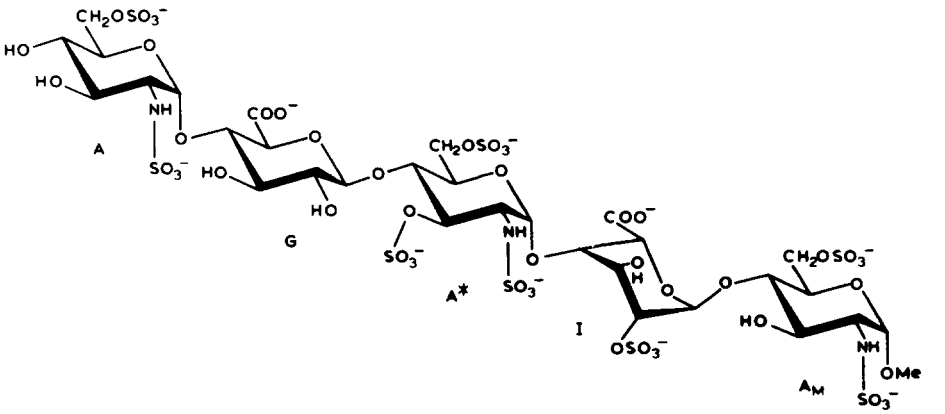

Scheme 1.

mechanics and molecular dynamics calculations [7h], [14]. Though this unique conformational flexibility could be relevant to the biological properties, the orientation of carboxyl and sulfated groups has also been discussed as being potentially important during the complexation of antithrombin III and pentasaccharide **I** [15]. In addition, more complex motional properties can be expected in **I** since, in a recent computational study [7h], several low energy minima were found on the Ramachandran-type two-dimensional (φ,ψ) map. In order to understand molecular details of the interaction of the pentasaccharide with antithrombin III, the dynamics in **I** in aqueous solutions should be fully characterized. In this paper, we present the results of an analysis of the overall and internal motions in **I** using ^{1}H and ^{13}C relaxation data obtained at various magnetic field strengths. Dipolar and CSA (chemical shift anisotropy) relaxation mechanisms are considered, as well as their cross-correlation. Data are analyzed within the model free approach [16] and the values of order parameters and the rates of internal motions are estimated.

2. Experimental methods

Sample.—Pentasaccharide [methyl *O*-(2-deoxy-2-sulfamido-6-*O*-sulfo-α-D-glucopyranosyl)-(1 → 4)-*O*-β-D-glucopyranosyluronic acid)-(1 → 4)-*O*-(2-deoxy-2-sulfamido-3,6-di-*O*-sulfo-α-D-glucopyranosyl)-(1 → 4)-*O*-(2-*O*-sulfo-α-L-idopyranosyluronic acid)-(1 → 4)-2-deoxy-2-sulfamido-6-*O*-sulfo-α-D-glucopyranoside decasodium salt; A-G-A*-I-A_M, **I**, Scheme 1] was synthesized as described previously [17]. The compound was purified by ion-exchange chromatography, lyophilized twice from D_2O, and finally dissolved in D_2O (99.996 atom% D_2O, low paramagnetic impurities) giving a ca. 5 mM solution; the solution pH was adjusted to 7. The solution in the NMR tube was purged with argon to remove oxygen and the tube was then sealed.

NMR Spectroscopy.—NMR spectra were recorded at 11.7 and 9.4 T on Bruker AMX 500 and AMX 400 spectrometers, respectively, and at 7 T on Bruker AC 300

spectrometer. The temperature of the sample in the spectrometer probe was maintained at 298 K in all measurements. In order to avoid spinning artefacts the sample was not spun.

Two-dimensional double-quantum-filtered COSY, [18] HMQC [19] and HMBC [20] spectra were collected with presaturation of the residual HDO signal. The first two experiments were recorded in the phase sensitive mode for quadrature detection in the ω_1 dimension using TPPI [21]. Two independent one-dimensional NOESY experiments at 500 and 400 MHz were acquired for each mixing time using Gaussian pulses for semiselective excitation of protons [22]. Mixing times varied from 200 up to 800 ms. The recycle time was 11 s (T_1 of the slowest relaxing proton A_3 was 2.12 s in **I**, determined by inversion recovery at 500 MHz, except for the OMe protons). Final digitization of the spectra was 0.1 Hz/Pt and exponential filtering was used before Fourier transformation. Two-dimensional $^1H-^{13}C$ correlation experiments with double INEPT transfer of coherence from protons to carbons and back to protons [3], modified for T_1 and T_2 measurements [4a] were used. The 2D spectra consisted of 512 t_1 real points and 1024 t2 real points; the quadrature detection in ω_1 was achieved with TPPI. Delays between pulses in the INEPT sequence were set to 1.66 ms (optimized for $^1J_{C\text{-}H} \approx 150$ Hz). Six different relaxation delays T were used in T_1 experiments, namely, 20, 70, 120, 200, 300, and 450 ms. In the T_2 experiments the CPMG [23] (Carr–Purcell–Meiboom–Gill) pulse trains were 6, 24, 48, 72, 96, 150, and 270 ms long. 2D spectra were zero-filled to 2K × 2K giving final digital resolution of 0.95 Hz/Pt in F2 and 3.0 Hz/Pt in F1. Lorenzian-to-Gaussian filtering functions were used prior to Fourier transformation and the cross-peak volumes were measured in each T_1 and T_2 experiment using the UXNMR software package running on a Bruker X32 computer. T_1 and T_2 relaxation times were also measured with modified sequences [24] to suppress the effect of cross-correlation between dipolar and chemical shift anisotropy relaxation mechanisms. T_1 and T_2 values were calculated from a two-parameter best fit to the experimental cross-peak volumes using the non-linear Levenburg–Marquart algorithm. Standard deviations of the fit were typically 1–2%, in cases where cross-correlation effects were neglected and the decays were fitted to a single-exponential, standard deviations varied between 3–8%. ^{13}C NMR longitudinal relaxation times were also measured at 7 T by the inversion recovery method. Broad-band-decoupled ^{13}C spectra with 10 τ values were accumulated with 15000 transients for each spectrum. Spin-lattice relaxation times were computed using a 3-parameter fit.

3. Analysis of the data

For the ^1H (spin I)–^{13}C (spin S) system relaxing by dipole–dipole and chemical shift anisotropy, the time dependence of the carbon longitudinal relaxation is [25,26]

$$d/dt[S_z(t)] = -[\sigma_{IS}\Delta I_z + (\rho_S + \rho_{CSA})\Delta S_z + \mu_{IS,S}2\Delta I_z S_z], \quad (1)$$

where Δ represents a deviation from thermal equilibrium. For ^{13}C spins, the spin-lattice relaxation rate is [25]

$$\rho_S = 1/10D^2[J(\omega_H - \omega_C) + 3J(\omega_C) + 6J(\omega_H + \omega_C)], \quad (2)$$

the chemical shift anisotropy term is [27]

$$\rho_{CSA} = 2/15C^2J(\omega_C), \tag{3}$$

and the cross-correlation term is [26]

$$\mu_{IS,S} = C^2D^2[6J(\omega_C)][0.5(3\cos^2\varphi - 1)], \tag{4}$$

and the cross-relaxation term is [25]

$$\sigma_{IS} = 1/10D^2[6J(\omega_H + \omega_C) - J(\omega_H - \omega_C)]. \tag{5}$$

Similar expressions exist for transverse relaxation rates [28]. D is the dipolar coupling constant $D = (\mu_o/4\pi)\gamma_H\gamma_C\hbar\langle r_{C\text{-}H}^{-3}\rangle$. Chemical shift anisotropy constant C is given by $C = \omega_C(\Delta\sigma)$, where $\Delta\sigma = \sigma_\parallel - \sigma_\perp$, and $\sigma_\parallel$ and $\sigma_\perp$ are the parallel and perpendicular components of chemical shift anisotropy tensor. φ is the angle between the principal axis of the cylindrically symmetric chemical shift tensor and the C–H relaxation vector.

The spectral density function $J_{IS}(\omega)$, (Eqs. 2–5) can have different forms depending on the nature of the overall and internal motions, and a number of expressions have been proposed [29]. In the model free approach [16], $J_{IS}(\omega)$ for an isotropically tumbling molecule has the form

$$J_{IS}(\omega) = \frac{S_{C-H}^2\tau_o}{1 + (\tau_o\omega)^2} + (1 - S_{C-H}^2)\frac{\tau}{1 + (\tau\omega)^2}, \tag{6}$$

where τ_o is the tumbling time of the molecule, $1/\tau = 1/\tau_o + 1/\tau_e$ and τ_e is the effective correlation time. $S_{C\text{-}H}^2$ is the generalized order parameter denoted by subscript for the C–H relaxation vector. If the molecule is tumbling anisotropically, and can be considered axially symmetric with two different diffusion coefficients parallel ($D_\parallel$), and perpendicular ($D_\perp$) [30], the resulting spectral density $J_{IS}(\omega)$ can be approximated in the form [4b]

$$J_{IS}(\omega) = S_{C-H}^2J_{an}(\omega) + (1 - S_{C-H}^2)\frac{\tau}{1 + (\tau\omega)}, \tag{7}$$

where

$$J_{an}(\omega) = 0.25(3cos^2\theta - 1)^2\tau_a/[1 + (\omega\tau_a)^2] + (3sin^2\cos^2\theta)\tau_b/[1 + (\omega\tau_b)^2] + 0.75(\sin^4\theta)\tau_c/[1 + (\omega\tau_c)^2]$$

and

$$\tau_a = \tau_\perp$$

$$1/\tau_b = 5/(6\tau_\perp) + 1/(6\tau_\parallel)$$

$$1/\tau_c = 1/(3\tau_\perp) + 2/(3\tau_\parallel)$$

and $\tau_\parallel = 1/6D_\parallel$ and $\tau_\perp = 1/6D_\perp$. $\tau_\parallel$ and $\tau_\perp$ are the correlation times for reorientation about the long and short axes, respectively; θ is the angle between the C–H relaxation vector and the symmetry axis. In the present case, we assumed that the main

axis is along the chain of the pentasaccharide connecting the C-1 and C-4 carbons in the pyranose units and glycosidic oxygens. Though the symmetric top model describes the overall molecular tumbling of the pentsaccharide more appropriately than the isotropic one, this model might be still rather simplistic to account for all details of overall motion of **I**. We used this model presently because we considered it as a reasonable compromise between the feasibility to derive the motional parameters (more complex models would require considerably more parameters to derive) and the fair physical description of the overall tumbling of the molecule in solution.

If one considers that fluctuations are not only in the orientation, but also in the internuclear distances (e.g., for protons), $J_{IS}(\omega)$ has the form [16]

$$J(\omega) = S^2_{H-H}\langle r^{-3}\rangle^2 J_{an} + \left[\langle r^{-6}\rangle - \langle r^{-3}\rangle^2 S^2_{H-H}\right]\frac{\tau}{1+(\omega\tau)^2}, \quad (8)$$

where $S^2_{H\text{-}H}$ denotes the generalized order paramenter for the H–H relaxation vector and τ_{eff} is the effective correlation time. Since, to a good approximation, angular and radial order parameters can be factorized [31,32]

$$S^{*2}_{H-H} = S^2_{H-H}\frac{\langle r^{-3}_{H-H}\rangle^2}{\langle r^{-6}_{H-H}\rangle}, \quad (9)$$

where $S^{*2}_{H\text{-}H}$ includes both angular ($S^2_{H\text{-}H}$) and radial ($\langle r^{-3}_{H\text{-}H}\rangle^2/\langle r^{-6}_{H\text{-}H}\rangle$) components of motional averaging, $J(\omega)$ can be expressed in the formally identical form as for relaxation through fixed distances

$$J_{IS}(\omega) = S^{*2}_{H-H}J_{an}(\omega) + (1 - S^{*2}_{H-H})\frac{\tau}{1+(\tau\omega)}.$$

Although the value of $S^2_{H\text{-}H}$ does not depend on the distance it can differ for the anisotropically tumbling molecule from that of the $S^2_{C\text{-}H}$ due to the various orientations of the H–H and C–H relaxation vectors in the molecule.

4. Results and discussion

The ^{1}H 500 MHz spectrum of the pentasaccharide **I** is shown in Fig. 1. The ^{1}H chemical shifts for all protons were determined by double-quantum-filtered COSY and are in agreement with those published [17a]. Both HMQC and HMBC experiments were used to assign ^{13}C resonances (Table 1). Three-bond proton–proton coupling constants confirmed the $^4C_1$ conformation of the D-pyranose units; for the L-iduronic acid both $^1C_4$ and $^2S_0$ conformers are present in solution [12b]. The two-dimensional double INEPT spectrum, obtained by pulse sequence for T_1 relaxation times measurements, is shown in Fig. 2. Two cross-peaks were overlapped, A2 and A_M2, and they were discarded from further analysis. Similarly, the cross-peak volumes for A* 2 and G2 were affected by t_1 noise of the strong OMe signal. Fig. 3 illustrates contour plots of the three subspectra collected with three different lengths of CPMG spin-echo. The cross-peak intensities decreased as a function of the relaxation interval. Partial overlap of the signals of G3,

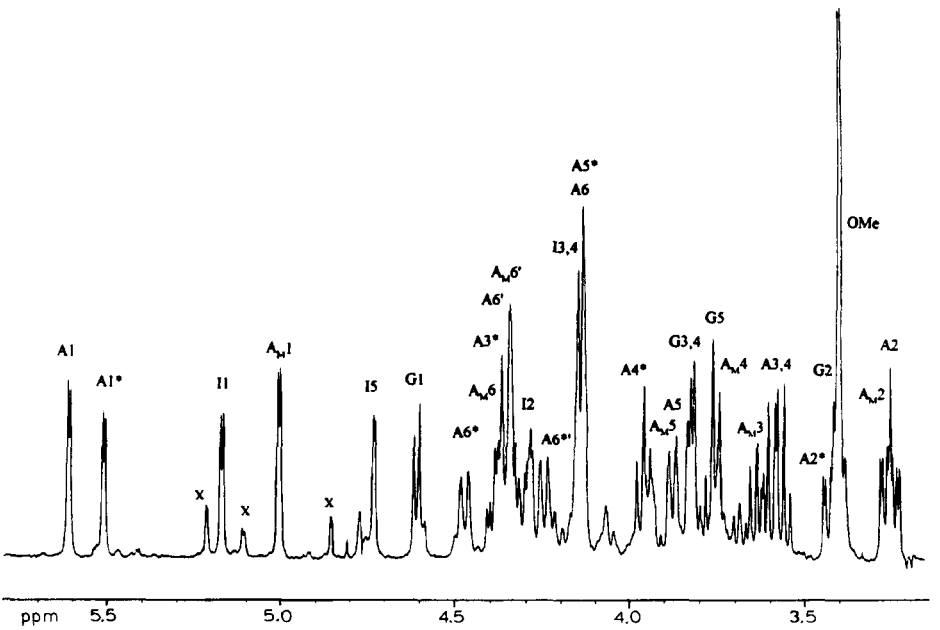

Fig. 1. ^{1}H 500 MHz NMR spectrum of the pentasaccharide **I** is aqueous solution. Chemical shifts are referenced to external DSS. x denotes signals corresponding to the partially desulfated units. Small spurious signal at 4.77 ppm originate from the residual HDO resonance.

G4, G5, and A_M4 resulted in higher values of standard deviations for the fit of the T_1 and T_2 relaxation times, however, quantitative analysis was still possible. Selected cross-sections from the two dimensional spectra and the computed curves of the magnetization decay for T_1 and T_2, and the experimental cross-peak volumes, are shown in Fig. 4.

Anisotropic tumbling and cross-correlation effects.—In the derivation of spin-lattice and spin-spin relaxation times from the spectral data, it is necessary to take into account all possible contributions to the relaxation rates R_1 and R_2, respectively. It is well known that the effect of the CSA may not be negligible at high fields [27]. In our case, for methine carbons in the pyranose rings, the values of the CSA tensor obtained for the secondary alcoholic group [33] can be considered relevant: $\sigma_{11} = 90$, $\sigma_{22} = 83$, and $\sigma_{33} = 42$ ppm, suggesting that the assumption of the axially symmetric tensor is reasonable and that the value of $\Delta\sigma = \sigma_{\parallel} - \sigma_{\perp} \approx -50$ ppm. This value gives the estimate for the CSA coupling constants: $C = 3.95 \times 10^4$ s^{-1} at 11.7 T. Though, from the comparison of the C value with the dipolar coupling constant ($D = 1.37 \times 10^5$ s^{-1}), the CSA contributes to the relaxation rates only by a fraction of R_1 (about 5%), we considered both interactions in further calculations to achieve greater precision of the derived relaxation times.

Spin-lattice (T_{1cc}) and spin-spin (T_{2cc}) relaxation times were computed from the relaxation data obtained with the pulse sequences where no suppression of the cross-correlation effects between dipolar and CSA relaxation mechanisms was made; the data are

Table 1
^{13}C NMR data for the pentasaccharide **I** in aqueous solution recorded at 298 K. Chemical shifts (δ, ppm, column 3) and relaxation times (in seconds): T_1 (column 4), recorded at 11.7 T without suppression of cross-correlation between dipolar and CSA relaxation mechanisms, T_1 (column 5), recorded at 11.7 T with suppression of cross-correlation, T_1 (column 6), recorded at 7 T with inversion recovery, T_2 (column 7), recorded at 11.7 T without suppression of cross-correlation between dipolar and CSA relaxation mechanisms, T_2 (column 8), recorded at 11.7 T with suppression of cross-correlation. Averaged values and standard deviations are listed in the last row for each residue

		δ (ppm)	$^{13}C\ T_{1cc}$ [11.7 T]	$^{13}C\ T_1$ [11.7 T]	13C T_1 [7 T]	$^{13}C\ T_{2cc}$ [11.7 T]	$^{13}C\ T_2$ [11.7 T]
A	C-1	99.65	0.33	0.29	0.21	0.24	0.16
	C-2	60.06	[a]	[a]	[a]	[a]	[a]
	C-3	73.21	0.32	0.29	[a]	0.24	0.17
	C-4	71.01	0.31	0.28	0.23	0.22	0.17
	C-5	71.79	0.31	0.28	[a]	0.23	0.17
	C-6	68.60			0.12		
			0.318(0.010)	0.285(0.006)		0.233(0.010)	0.168(0.005)
G	C-1	103.30	0.28	0.25	0.19	0.25	0.18
	C-2	74.84	[a]	[a]	[a]	[a]	[a]
	C-3	78.17	0.29	0.26	[a]	0.24	0.19
	C-4	78.91	0.30	0.26	[a]	0.22	0.18
	C-5	79.14	0.30	0.26	[a]	0.22	0.17
			0.293(0.010)	0.258(0.005)		0.233(0.015)	0.180(0.008)
A*	C-1	98.13	0.27	0.22	0.16	0.19	0.16
	C-2	58.74	[a]	[a]	0.16	[a]	[a]
	C-3	78.26	0.28	0.23	[a]	0.21	0.17
	C-4	74.90	0.25	0.23	[a]	0.20	0.18
	C-5	71.61	0.26	0.23	[a]	0.22	0.17
	C-6	68.31			0.11		
			0.265(0.013)	0.228(0.005)		0.205(0.013)	0.170(0.008)
I	C-1	101.68	0.28	0.25	0.19	0.18	0.14
	C-2	79.40	0.29	0.25	0.18	0.21	0.17
	C-3	72.50	0.29	0.24	[a]	0.21	0.17
	C-4	78.12	0.30	0.26	[a]	0.21	0.18
	C-5	72.43	0.28	0.24	[a]	0.20	0.17
			0.288(0.008)	0.248(0.008)		0.202(0.013)	0.166(0.015)
A_M	C-1	100.29	0.34	0.28	0.24	0.23	0.16
	C-2	59.79	[a]	[a]	[a]	[a]	[a]
	C-3	71.85	0.35	0.30	[a]	0.24	0.18
	C-4	78.37	0.36	0.30	[a]	0.24	0.18
	C-5	70.60	0.34	0.30	0.23	0.23	0.17
	C-6	69.05			0.13		
			0.348(0.010)	0.295(0.010)		0.235(0.006)	0.173(0.010)

[a] Not determined due to overlap.

listed in Table 1 (columns 4 and 7). T_{1cc} varied from 0.25 up to 0.35 s at 11.7 T depending on the saccharide unit. The shorter T_{1cc} relaxation times were in the central A* residue, the longer towards both ends of the molecule. A similar trend was observed also at 7 T (the spectra recorded with inversion recovery method); however, these data are much poorer due to overlap of the ^{13}C resonances and may also be more affected by

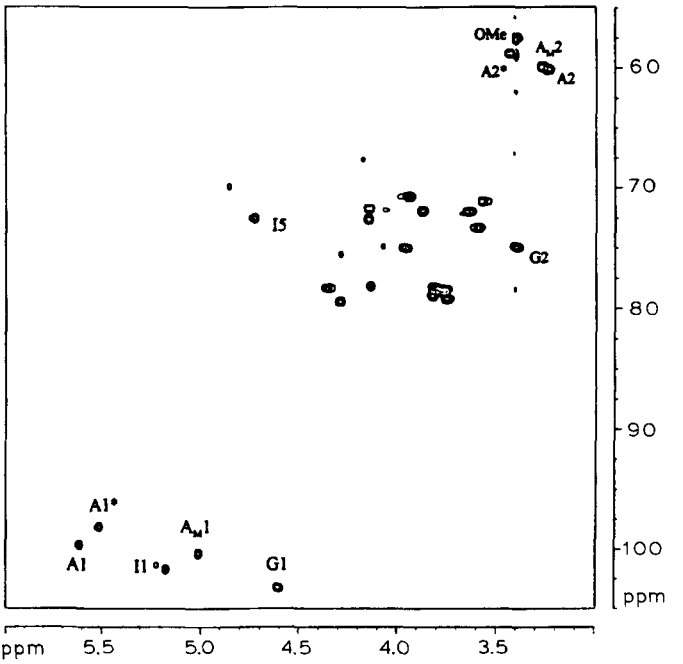

Fig. 2. Two-dimensional $^{1}H-^{13}C$ double INEPT spectrum of the pentasaccharide at natural abundance in aqueous solution collected with a pulse sequence for T_1 relaxation time measurement with T = 20 ms. The total measurement time was ca. 28 h. Assignment is given for the anomeric carbons and part of the ring carbons. The assignment of other ring carbons is shown in Fig. 3. for clarity.

the lower signal to noise ratio. Averaged values and standard deviations were calculated for each unit from the individual carbons and are listed in the last row for each residue in Table 1. The differences between the values of T_{1cc} for the various residues are outside the standard deviations and indicate that the molecule tumbles anisotropically. In

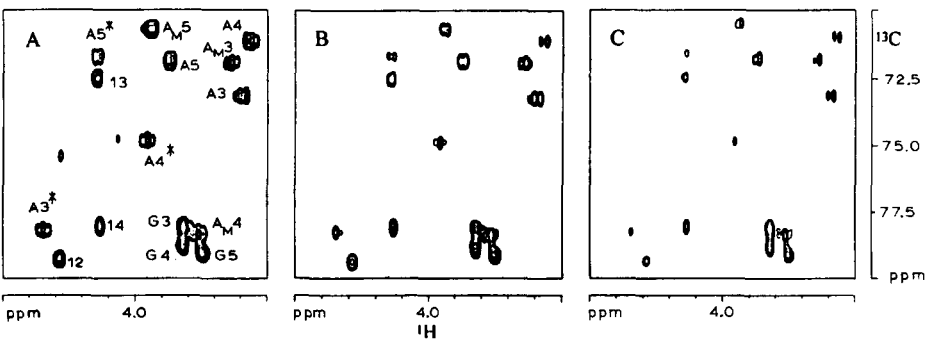

Fig. 3. Contour plots of the ring carbons region of the double INEPT spectra recorded with the pulse sequence for T_2 measurement with different lengths of CPMG pulse train: 6 (A), 150 (B), and 270 ms (C). Cross-peaks at 4.28 and 4.07 ppm originate from impurities.

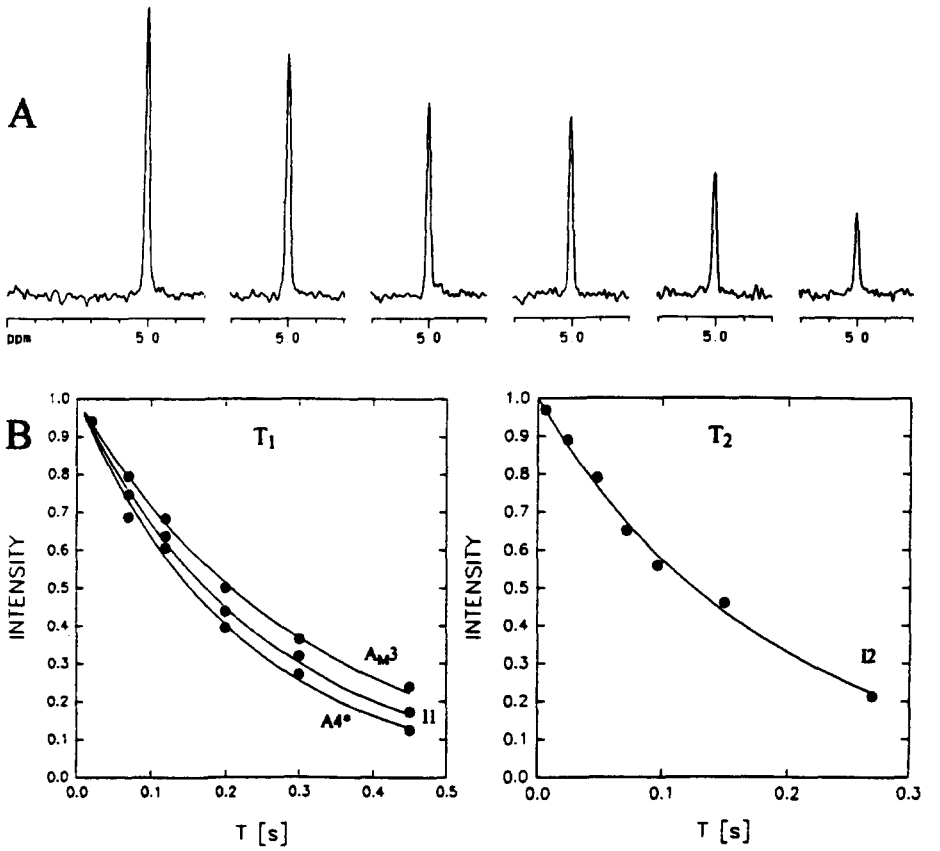

Fig. 4. (A) Cross-sections from the two dimensional spectra parallel to the ω_2 axis through the A_M1 signal using the pulse scheme for the measurement of T_1 relaxation times. Recorded with 6 different lengths of T delays: 20, 70, 120, 200, 300, and 450 ms. (B) Experimental ^{13}C T_1 and T_2 curves for selected signals. Points represent normalized intensities of the cross-peaks, solid lines are the single-exponential fits of the data. For T_1, three different curves are shown, corresponding to various values of T_1: A_M3 (0.34 s), I1 (0.25 s), and A4* (0.23 s).

what follows, we shall consider the molecule as the axially symmetric one with two diffusion constants $D_{\|}$ and $D_{\perp}$, where $D_{\|} > D_{\perp}$. However, the numerical values of T_1 are only approximate since the experimental data for each carbon were fitted to a single exponential, neglecting the effect of cross-correlation. The values of T_1 and T_2 relaxation times, respectively obtained by pulse sequences that remove the effect of cross-correlation between dipolar and CSA mechanisms [24], are shown in Table 1, columns 5 and 8. The values of T_1 varied from 0.22 to 0.30 s, T_2 were between 0.14 and 0.19 s. The difference between T_{1cc} and T_1 in the pentasaccharide **I** was 10–15%, for T_2 the difference was 20–25%, well outside the experimental error [34]. Similar differences in relaxation times have been described for protein molecules [24,35]. It has been shown theoretically [26,36], as well as experimentally [24,35a], that interference effects can

influence the T_2 values up to 25–30%; for the longitudinal relaxation times the effects observed were 5–8%. However, since the interference effect depends on the molecular tumbling time it can be expected that for medium-sized molecules the influence can be more significant also for T_1 values. The measured difference in the longitudinal relaxation times in **I** was 10–15%. Thus, in the region of T_1 minimum, where the proton spin-flip rate is slow and the relaxation rate is high, interference effects can exceed 10% also in the longitudinal relaxation times. For small molecules at room temperature where $\omega\tau_0 \ll 1$ and the relaxation rates are slow, the influence of cross-correlation can be expected to be within the experimental error.

The numerical values for T_1 in different residues agree with the assumption of an anisotropically tumbling molecule, for the A* residue $T_1 = 0.23$ s, for the terminal units $T_1 = 0.29$ and 0.30 s, respectively. However, in this case the anisotropic tumbling should also affect the spin-spin relaxation rates; consequently, the values of T_2 can be expected to be shorter for the terminal residues. For example, if we compare transverse relaxation times for the rigid, isotropically tumbling molecule with $\tau_0 = 0.6$ ns (the value of overall tumbling is close to the T_1 minimum region according to the T_1 values) with the rigid molecule tumbling anisotropically with $\tau_\perp/\tau_\parallel = 3.3$ ($\tau_\parallel = 0.6$ ns) we get the difference between T_2 relaxation times of about 40 ms ($T_{2iso} \sim 0.17$ s, $T_{2aniso} \sim 0.13$ s). However, as we found in T_1 and T_2 data generated for a wide range of values of, $\tau_\parallel$, $\tau_\perp$, $\tau_\perp/\tau_\parallel$, S^2 and τ_e, the magnitudes of the T_2 values can be compensated with internal motions. Thus, for example, for $S^2 \sim 0.7$ and $\tau_\perp/\tau_\parallel = 3.3$ (see later analysis; this holds for a relatively wide range of values of $\tau_\perp/\tau_\parallel$ and S^2) transverse relaxation times are equal ($T_{2aniso} \sim 0.17$ s) to those for the rigid, isotropically tumbling molecule. Therefore the constant T_2 values for all residues are in agreement with the anisotropically tumbling molecule, however, with $S^2 < 1$.

Proton cross-relaxation rates.—One-dimensional NOESY spectra when spin of the A1* proton was inverted, collected at 11.7 T and 9.4 T with 400 ms mixing time, are shown in Fig. 5. One intra-ring NOE was observed on the A2* and two inter-ring NOEs on I3 and I4. Similarly, when spin of the A4* proton was inverted, one intra-ring NOE on the A2* was observed and one inter-ring on the G1. Numerical values of the NOEs and the ratios of the cross-relaxation rates $\sigma_{500}/\sigma_{400}$ are listed in Table 2. Comparison of the cross-relaxation rates of protons relaxing through the 'rigid' distances within the monosaccharide unit, i.e., A1*–A2*, and A4*–A2* is of interest. The computed distances are A1*–A2* = 248 pm, A2*–A4* = 245 pm in the A* monosaccharide (methyl glycoside) in aqueous solution obtained by the Macromodel program [37] using the MM2 force field. The cross-relaxation rates derived from the experimental data at 11.7 T are A1*–A2* = −0.126 s^{-1} ($\sigma_{1\text{-}2}(500)$) and A2*–A4* = −0.061 s^{-1} ($\sigma_{2\text{-}4}(500)$), thus $\sigma_{2\text{-}4}(500)$ is about half the $\sigma_{1\text{-}2}(500)$ though the distances are nearly the same. The correlation times corresponding to these cross-relaxation rates, using the spectral density for an isotropically tumbling rigid molecule, are 810 ps for the A1*–A2* relaxation vector and 520 ps for the A2*–A4* relaxation vector, respectively. Thus, correlation times obtained from two relaxation vectors with different orientation (the angle A1*–A2*–A4* is about 109°) are quite different, supporting the earlier conclusion (based on the ^{13}C T_1 data) about the anisotropic tumbling of the pentasaccharide. The same is valid for the ratios of the cross-relaxation rates collected at

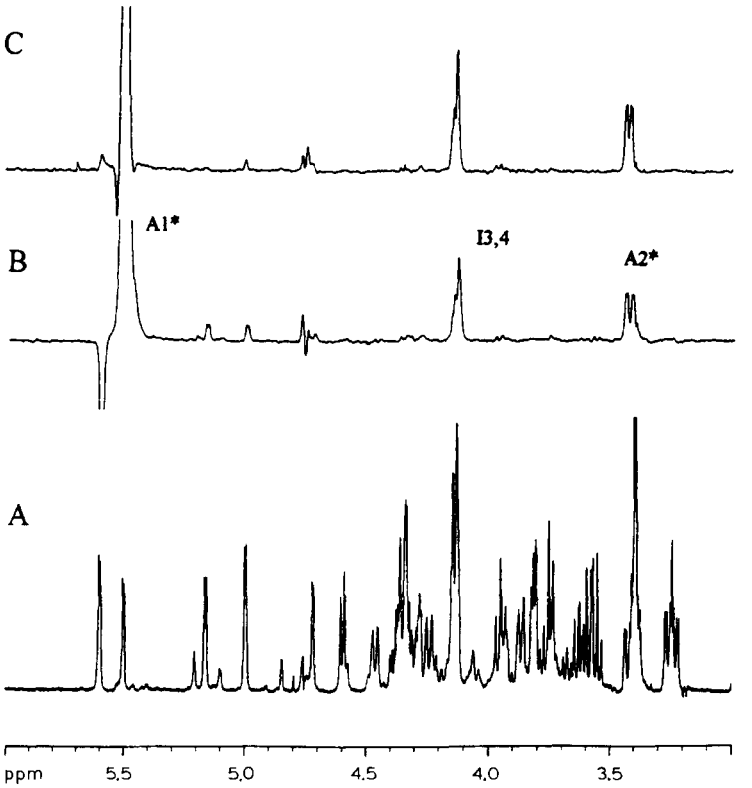

Fig. 5. One dimensional NOESY spectra of the pentasaccharide when the spin of the A1* was inverted, collected with 400 ms mixing time at two different magnetic fields. Small spurious signals at 4.77 ppm in all three spectra originate from the residual HDO resonance. (A) ^{1}H 500 MHz spectrum of I, (B) 1D NOESY spectrum recorded at 9.4 T, and (C) 1D NOESY spectrum recorded at 11.7 T.

two field strengths; consequently in this case the ratio cannot be used to detect internal motion on the glycosidic linkage as in our previous study [8] since the relaxation data could be more affected by overall anisotropic motion than by internal motions. Moreover, since several protons are tightly coupled in the molecule (e.g., I3 and I4, G3 and G4) [12b] the NOEs across the glycosidic linkages A1*–I3 + I4 and A4*–G1, (and the corresponding ratios $\sigma_{500}/\sigma_{400}$ as well) are affected by strong coupling [38]. Similarly, particularly for the NOE between the A4* and G1 across the glycosidic linkage, the detected NOEs for different mixing times are very small (0.5–1.5% at 9.4 T) and, consequently, experimental error can be high due to low signal to noise ratio. For the above reasons, the NOEs across the glycosidic linkage were discarded. The effect of correlated cross-relaxation was assumed to be negligible since our analysis of the NOEs was limited to short mixing times [29a],[39].

Numerical analysis.—In order to characterize the motional properties of **I** in aqueous solution in a more quantitative way the model free parameters [16] were calculated. In the first step, we generated the values of T_1 (500), T_2 (500), T_1 (300), σ(500) and

Table 2
Transient NOEs (%) recorded at 11.7 T (σ_{500}) and at 9.4 T (σ_{400}) at 298 K in aqueous solution. Spins of the protons A1* and A4* were inverted in the central unit in the pentasaccharide (A-G-A*-I-A_M). In the last column the ratios of the transient NOEs ($\sigma_{500}/\sigma_{400}$) measured at two different field strengths are listed

	$\omega/2\pi$ 500 MHz		$\omega/2\pi$ 400 MHz		$\sigma_{500}/\sigma_{400}$	
A1* irrad.	σ_{500}		σ_{400}			
mixing time (ms)	A2*	I4+I3	A2*	I4+I3	A2*	I4+I3
200	3.2(0.15)	4.1(0.15)	2.7(0.10)	3.1(0.10)	1.2	1.4
400	6.2(0.10)	7.7(0.05)	5.0(0.05)	5.6(0.10)	1.2	1.4
600	10.0(0.10)	12.1(0.15)	7.5(0.15)	8.1(0.15)	1.3	1.5
800	13.1(0.20)	16.0(0.15)	10.1(0.15)	10.6(0.20)	1.3	1.5
A4* irrad.	A2*	G1	A2*	G1	A2*	G1
mixing time (ms)						
200	1.2 [a]	0.9 [a]	0.8(0.10)	0.4(0.15)	1.5	2.1
400	2.4(0.10)	1.7(0.10)	1.6(0.15)	0.9(0.10)	1.5	1.9
600	3.8(0.10)	2.4(0.20)	2.4(0.10)	1.2(0.15)	1.6	2.0
800	4.8(0.20)	3.3(0.10)	3.1(0.20)	1.6(0.20)	1.6	2.1

[a] Values of a single measurement at 500 MHz. Averaged values from two measurements are listed. The difference between the averaged and the experimental values is in parenthesis.

$\sigma(400)$ for a wide range of values of $\tau_{\|}$, $\tau_{\perp}$, τ_e, $S^2_{C\text{-}H}$, $S^2_{H\text{-}H}$ and θ using the equations given in the Methods section. The approximate magnitudes of the parameters for the A* residue were $\tau_{\|} \sim 450$ ps, $\tau_{\perp} \sim 1.6$ ns, $S^2 \sim 0.8$, and $\theta \sim 90°$. Then we minimized the function [40]

$$f(S,\tau) = \left[(T_{1expt} - T_{1calcd})/T_{1expt}\right]^2 + \left[(T_{2expt} - T_{2calcd})/T_{2expt}\right]^2 + \Sigma\left[\left[(\sigma_{500expt} - \sigma_{500calcd})/\sigma_{500expt}\right]^2 + \left[(\sigma_{400expt} - \sigma_{400calcd})/\sigma_{400expt}\right]^2\right] \quad (11)$$

where T,σ_{expt} are the experimental values and T,σ_{calcd} are the computed values; σ was used for both relaxation vectors A1*–A2* and A2*–A4*. The optimized values found from fitting the function are (Table 3): $\tau_{\|} = 450$ (20) ps, $\tau_{\perp} = 1.48$ (0.08) ns, $\tau_e = 50$ (82) ps, $S^2_{C\text{-}H} = 0.91(0.03)$, $S^2_{H\text{-}H} = 0.74(0.04)$ for the A1*–A2*, $S^2_{H\text{-}H} = 0.37(0.12)$ for

Table 3
Computed values of the effective correlation times τ_e, (ps/rad) order parameters $S^2_{C\text{-}H}$ for the pentasaccharide I

	τ_e	$S^2_{C\text{-}H}$
A	31(35)	0.72(0.10)
G	32(49)	0.85(0.05)
A*	50(85)	0.91(0.03)
I	28(51)	0.83(0.08)
A_M	15(25)	0.70(0.04)

the A2*–A4*; $\theta = 83°(5)$. The largest standard deviation (given in brackets) of the fit was found for the τ_e (more than 100%), this is probably the consequence of the high values of the order parameters [4c]. Furthermore, if we take into account the experimental error of the data, the value of the computed τ_e is even less precisely determined and consequently, should be taken to be in the range of tens of picoseconds. It is also of interest that order parameters have different values for various relaxation vectors A1*–A2*, A2*–A4*, and C–H within the same residue as a consequence of anisotropic tumbling with the C–H relaxation vector ($S^2_{C\text{-}H} = 0.91$) as being the most restricted in motional freedom. The model free parameters for other residues (Table 3) in the pentasaccharide were then obtained by fitting the experimental ^{13}C data (Eq. 11), where only a portion (for T_1 and T_2 at 11.7 T) of the right hand side of Eq. 11 was considered. The values of $\tau_{\|}$, $\tau_{\perp}$ and used were the same as for the A* unit. The decrease of the $S^2_{C\text{-}H}$ parameter from $S^2_{C\text{-}H} \sim 0.9$ to $S^2_{C\text{-}H} \sim 0.7$ reflects a higher degree of motion in the terminal residues. These data support conclusions of the recent theoretical analysis of **I** [7h] where several minima were found on the energy surface. The I-A_M part of the molecule was found to be more flexible, the A-G-A* part more restricted. Generalized order parameters derived from the experimental data show that there is no significant difference in the spatial restriction at both ends of the molecule. The values of the τ_e are smaller for the terminal residues, however, within the same order throughout the molecule. In addition, in the theoretical study, differences between the computed (obtained with spectral density function for isotropic motion) and experimental steady-state NOEs have been observed in several cases. The variations were detected for the enhancements across the glycosidic linkages and also within the same monosaccharide units. The anisotropic molecular tumbling of **I** observed in our study suggests a possible explanation for the discrepances described. The present experimental data thus complement the above mentioned theoretical study [7h] estimate the rate of internal motions and more appropriately characterize the overall tumbling of the pentasaccharide. Other independent evidence of internal motion on the glycosidic linkages could be found in the theoretical interpretation of the temperature dependence of the three-bond proton carbon coupling constants across the glycosidic linkage [7a] and the one-bond proton carbon coupling constants [41], however, this was not within the aim of our study. Based on the present experimental data exclusively, it is not possible to derive the geometry of individual conformers involved in the averaging process and to compare the results with the published data. The more detailed comparison would require molecular dynamics simulations and the analysis of the trajectories and computation of the inter-proton distances and the correlation functions.

Recently, we have studied internal motions in two disaccharides using the relaxation data collected at various magnetic field strengths [8]. We have concluded that if protons are cross-relaxing through fluctuating distances, the correlation times derived from the ratio of such cross-relaxation rates, measured at various frequences, can be different compared to the tumbling times calculated from the ^{13}C T_1 data. This is a consequence of the fact that the radial component ($\langle r^{-3}_{H\text{-}H}\rangle^2 / \langle r^{-6}_{H\text{-}H}\rangle$) of the order parameter S^{*2} differs from unity (Eq.9). Moreover, as seen from the present study, similar discrepancies can be obtained when the molecule is tumbling anisotropically in solution. In such a case, the appropriate spectral density function should be considered, as well as order

parameters calculated for the different relaxation vectors in the molecule. In addition to both arguments, the derived tumbling times from the experimental data can be affected by cross-correlation effects as well. Since, as was shown for the pentasaccharide, the interference effects between dipolar and CSA mechanisms can have an influence of up to 10–15% in T_1 and 20–25% in T_2 relaxation times, the corresponding difference between the correct and the affected relaxation times is also reflected in computed correlation times from the ^{13}C relaxation data, if no suppression of these effects is carried out.

5. Conclusions

We have demonstrated, based on both heteronuclear and homonuclear relaxation data collected at various magnetic field strengths, that pentasaccharide **I** has a relatively complex motional behaviour in aqueous solution. It seems reasonable to adopt the symmetric top model to describe the overall molecular tumbling, however, the presence of internal motions must also be included in the analysis to interpret the experimental data. The model free analysis showed that the rate of internal motions is on a picosecond timescale and that order parameters decrease from the central residue towards both ends of the molecule. The analysis also showed that order parameters can differ for the various relaxation vectors, depending on their orientation in the molecule as a consequence of anisotropic tumbling. Moreover, it has been found that cross-correlation between dipolar and CSA relaxation mechanisms contributes significantly to the relaxation rates. Thus, the data presented show that for a more precise interpretation of the relaxation data of **I**, not only must consideration be given to internal motions and to anisotropic tumbling, but to effects of cross-correlation as well.

Acknowledgements

Authors are indebted to Professor B. Casu for discussions, Dr. M. Guerrini for collaboration, and Dr. M. Petitou for providing the pentasaccharide sample.

References

[1] D. Neuhaus and M. Williamson, *The Nuclear Overhauser Effect in Structural and Conformational Analysis*, VCH, Weinheim, 1989.
[2] W.P. Aue, E. Bartholdi, and R.R. Ernst, *J. Chem. Phys.*, 64 (1976) 2229–2246.
[3] G. Bodenhausen and D.J. Ruben, *Chem. Phys. Lett.*, 69 (1980) 185–188.
[4] (a) L.E. Kay, D.A. Torchia, and A. Bax, *Biochemistry*, 28 (1989) 8972–8979; (b) G. Barbato, M. Ikura, L.E. Kay, R.W. Pastor, and A. Bax, *Biochemistry*, 31 (1992) 5269–5278; (c) A.G. Palmer III, M. Rance, and P.E. Wright, *J. Am. Chem. Soc.*, 113 (1991) 4371–4380; (d) A.J. Duben and W.C. Hutton, *J. Am. Chem. Soc.*, 112 (1990) 5917–5924.
[5] (a) J.R. Brisson and J.P. Carver, *Biochemistry*, 22 (1983) 1362–1368; (b) P. Dais and A.S. Perlin, *Carbohydr. Res.*, 194 (1989) 288–295; (c) P. Fernandez and J.J. Barbero, *Carbohydr. Res.*, 248 (1993)

15–36; (d) S.W. Homans and M. Foster, *Glycobiology,* 2 (1992) 143–151; (e) C.H. Penhoat, A. Imberty, N. Roques, V. Michon, J. Mentech, G. Descotes, and S. Pérez, *J. Am. Chem. Soc.,* 113 (1991) 3720–3727; (f) T. Peters and T. Weimar, *J. Biomol. NMR,* 4 (1994) 96–116; (g) L. Szilágyi and P. Forgó, *Carbohydr. Res.,* 247 (1993) 129–144; (h) W. Sicinska, B. Adams, and L. Lerner, *ibid.*, 242 (1993) 29–51; (i) A.L. Waterhause, T.M. Calub, and A.D. French, *ibid.*, 217 (1991) 29–42; (j) M. Zsiska and B. Meyer, *ibid.*, 243 (1993) 225–258.

[6] (a) C.J. Edge, V.C. Singh, R. Bazzo, G.L. Taylor, R.A. Dwek, and T.W. Rademacher, *Biochemistry,* 29 (1990) 1971–1974; (b) E.F. Hounsell, N.J. Jones, H.C. Gooi, T. Feizi, A.S.R. Donald, and J. Feeney, *Carbohydr. Res.,* 178 (1988) 67–78; (c) L.M.J. Kroon-Batenburg, J. Kroon, B.R. Leeflang, and J.F.G. Vliegenthart, *ibid.*, 245 (1993) 21–42.

[7] (a) M. Hricovíni, I. Tvaroška, and J. Hirsch, *Carbohydr. Res.,* 198 (1990) 193–203; (b) D.A. Cumming and J.P. Carver, *Biochemistry,* 26 (1987) 6664–6676; (c) A. Ejchart and J. Dabrowski, *Magn. Reson. Chem.,* 30 (1992) S115–S124; (d) A. Imberty, S. Perez, M. Hricovíni, R.N. Shah, and J.P. Carver, *Int. J. Biol. Macromol.,* 15 (1993) 17–23. (e) T. Kozár, F. Petrák, Z. Galová, and I. Tvaroška, *Carbohydr. Res.,* 204 (1990) 27–36; (f) C. Meyer, S. Perez, C.H. Penhoat, and V. Michon, *J. Am. Chem. Soc.,* 115 (1993) 10300–10310; (g) L. Poppe and H. van Halbeek, *J. Am. Chem. Soc.,* 114 (1992) 1092–1094; (h) M. Ragazzi, D.R. Ferro, B. Perly, P. Sinaÿ, P.M. Petitou, and J. Choay, *Carbohydr. Res.,* 195 (1990) 169–185.

[8] M. Hricovíni, R.N. Shah, and J.P. Carver, *Biochemistry,* 31 (1992) 10018–10023.

[9] (a) B. Casu, *Adv. Carbohydr. Chem. Biochem.,* 43 (1985) 51–134; (b) L.A. Fransson, in G.O. Aspinall (Ed.), *The Polysaccharides,* Vol. 3, Academic Press, London, 1985, pp 337–415.

[10] M. Hook, I. Bjork, J. Hopwood, and U. Lindhal, *FEBS Lett.,* 66 (1976) 90–93.

[11] (a) G. Gatti, B. Casu, G. Torri, and J.R. Vercellotti, *Carbohydr. Res.,* 68 (1979) c3–c7; (b) D.A. Rees, E.R. Morris, J.F. Stoddart, and E.S. Stevens, *Nature (London),* 317 (1985) 480.

[12] (a) B. Casu, J. Choay, D.R. Ferro, G. Gatti, J.C. Jacquinet, M. Petitou, A. Provasoli, M. Ragazzi, P. Sinaÿ, and G. Torri, *Nature (London),* 322 (1986) 215–216; (b) D.R. Ferro, A. Provasoli, M. Ragazzi, G. Torri, B. Casu, G. Gatti, J.C. Jacquinet, P. Sinaÿ, M. Petitou, J. Choay, *J. Am. Chem. Soc.,* 108 (1986) 6773–6778; (c) G. Torri, G., B. Casu, G. Gatti, M. Petitou, J. Choay, J.C. Jacquinet, and P. Sinaÿ, *Biochem. Biophys. Res. Commun.,* 128 (1985) 134–140.

[13] M. Ragazzi, D.R. Ferro, B. Perly, G. Torri, B. Casu, P. Sinaÿ, M. Petitou, and J. Choay, *Carbohydr. Res.,* 165 (1987) c1–c5.

[14] (a) B. Mulloy, M.J. Forster, C. Jones, and D.B. Davies, *Biochem. J.,* 293 (1993) 849–858; (b) M.J. Forster and B. Mulloy, *Biopolymers,* 33 (1993) 575–588.

[15] P.D.J. Grootenhuis and C.A.A. van Boeckel, *J. Am. Chem. Soc.,* 113 (1991) 2743–2747.

[16] G. Lipari and A. Szabo, *J. Am. Chem. Soc.,* 104 (1982) 4546–4559.

[17] (a) M. Petitou, P. Duchaussoy, I. Lederman, J. Choay, J.C. Jacquinet, P. Sinaÿ, and G. Torri, *Carbohydr. Res.,* 167 (1987) 67–75; (b) J. Choay, M. Petitou, J.C. Lormeau, P. Sinaÿ, B. Casu, and G. Gatti, *Biochem. Biophys. Res. Commun.,* 116 (1983) 492–499.

[18] U. Piantini, O.W. Sorensen, and R.R. Ernst, *J. Am. Chem. Soc.,* 104 (1982) 6800–6801.

[19] A. Bax and S. Subramanian, *J. Magn. Reson.,* 67 (1986) 565–569.

[20] A. Bax and M.F. Summers, *J. Am. Chem. Soc.,* 108 (1986) 2093–2094.

[21] D. Marion and K. Wuthrich, *Biochem. Biophys. Res. Commun.,* 113 (1983) 967–974.

[22] H. Kessler, S. Mronga, and G. Gemmecker, *Magn. Reson. Chem.,* 29 (1991) 527–557.

[23] (a) H.Y. Carr and E.M. Purcell, *Phys. Rev.,* 94 (1954) 630–638; (b) S. Meiboom and D. Gill, *Rev. Sci. Instrum.,* 29 (1958) 688–691.

[24] L.E. Kay, L.K. Nicholson, F. Delaglio, A. Bax, and D.A. Torchia, *J. Magn. Reson.,* 97 (1992) 359–375.

[25] I. Solomon, *Phys. Rev.,* 55 (1955) 559–565.

[26] L.G. Werbelow and D.M. Grant, *Adv. Magn. Reson.,* 9 (1977) 189–299.

[27] A. Abragam, *The Principles of Nuclear Magnetism,* Clarendon Press, Oxford, 1961.

[28] M. Goldman, *J. Magn. Reson.,* 60 (1984) 437–452.

[29] (a) J. Tropp, *J. Chem. Phys.,* 72 (1980) 6035–6043; (b) D.E. Woessner, *J. Chem. Phys.,* 37 (1962) 647–654.

[30] P.S. Hubbard, *J. Chem. Phys.,* 52 (1970) 563.

[31] P.O. Westlund and R.M. Lynden-Bell, *J. Magn. Reson.,* 72 (1987) 522–531.

[32] R. Bruschweiler, B. Roux, M. Blackledge, C. Griesinger, M. Karplus, and R.R. Ernst, *J. Am. Chem. Soc.*, 114 (1992) 2289–2302.
[33] F.A. Bovey, *Nuclear Magnetic Resonance Spectroscopy*, Academic Press, New York, 1980.
[34] M. Hricovíni and G. Torri, *Chem. Pap.*, 48 (1994) 211–213.
[35] (a) J. Boyd, U. Hommel, and I.D. Campbell, *Chem. Phys. Lett.*, 175 (1990) 477–482; (b) C. Dalvit and G. Bodenhausen, *Chem. Phys. Lett.*, 161 (1989) 554–560; (c) L. Di Bari, J. Kowalewski, and G. Bodenhausen, *J. Chem. Phys.*, 93 (1990) 7698–7705.
[36] R.L. Vold and R.R. Vold, *Prog. NMR Spectrosc.*, 12 (1978) 79–134.
[37] F. Mohamadi, N.G.J. Richards, W.C. Guida, R. Liskamp, C. Caufield, G. Chang, T. Hendrickson, and W.C. Still, *J. Comput. Chem.*, 11 (1990) 440–467.
[38] J. Keeler, D. Neuhaus, and M.P. Williamson, *J. Magn. Reson.*, 73 (1987) 45–68.
[39] T. Bull, *J. Magn. Reson.*, 72 (1987) 397–413.
[40] M.J. Dellwo and A.J. Wand, *J. Am. Chem. Soc.*, 111 (1989) 4571–4578.
[41] M. Hricovíni and I. Tvaroška, *Magn. Reson. Chem.*, 28 (1990) 862–866.